International Journal of Innovative Technology and Exploring Engineering (IJITEE)
ISSN: 2278-3075 (Online), Volume-8 Issue-11, September 2019

Segmentation of Human Spermatozoa using Threshold-Based Image Segmentation

L.Prabaharan, A. Sivapathi, A. Raghunathan

Abstract: ***The role of image processing in processing and analyzing the microscopic medical images is the most challenging and required task in the assisted method of fertilization for human society. The Human eye evaluation for the process of detecting the defective spermatozoa from the sample semen smear using the microscope yields subjective results, which may vary from person to person. The objective evaluation is based on an automated computer program segments the portion of interest from the image based on segmentation techniques. The effective segmentation in the medical image is to highlight the expected portions such as head, tail, and mid-piece for the further process of analyzing the defects in the sperm cell. Cluster-based image segmentation is one of the effective methods to segment the object from the background in the microscopic medical images [1]. Entropic thresholding techniques also had an impact on the segmentation of medical images [2]. We have implemented the various threshold based image segmentation and compared their results with the help of segmentation metrics and showed the effectiveness of thresholding techniques for microscopic medical images.***

Keywords: Segmentation, spermatozoa, Threshold, Entropy

I. INTRODUCTION

Analyzing the morphology of human spermatozoa in the sample semen smear, using a microscope is a kind of manual evaluation being followed for the determination of male factor infertility [3]. The role of image processing in medical image analysis gives the objective result, which would be the better process than the manual review [4]. The sperm cell images are taken with the help of high definition camera attached with the microscope and can be stored in bitmap format for the further image processing. The automated computer aided diagnostic system is influenced with the segmentation-process. Determining the failure or success of an automated analysis system is based on accurate segmentation [5]. Image processing techniques are being used for the past twenty years in the microscopic medical image field, which gives fruitful result to the researchers. The authors of [6] and [7] have applied image segmentation techniques and classification on cancer cells. Image segmentation techniques were implemented for the blood cell analysis in [8] and [9]. Segmentation process was most notable for other microscopic medical image applications include muscle cells [10] and brain cells [11]. The thresholding is a simple segmentation method, in [12] the new local thresholding segmentation was proposed for a microscopic image and solved the problem of non-uniform distribution of staining. Fig.:1 presents an example of Normal sperm cell Fig.:1(a) and Abnormal sperm cell image Fig.:1(b) taken from the gold-standard database available online [18].

The abnormality is a morphological defect appear on any portion of the spermatozoon. It is a defect on head, mid-piece, and tail in the sperm cell. The defective sperm cells may decrease the success ratio in the assisted method of fertilization.

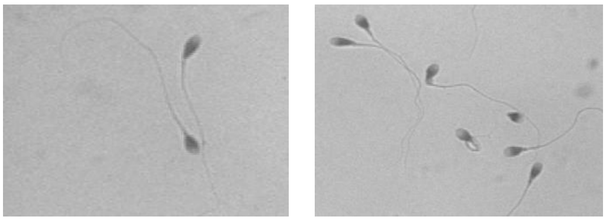

(a) Normal sperm cell (b) Abnormal sperm cell

Fig.:1 Spermatozoa cells

The segmentation of human spermatozoa is to find the boundaries of various parts in the sperm cells such as head, mid-piece, and tail. It is the process of dividing the image into indivisible divisions. The pixels belonging to every division is almost related to each other. The aim of segmentation is to increase the homogeneity among the pixels in every segment and increase the heterogeneity between the segments, such that accuracy can be improved in the segmentation process. Image segmentation has been used in many biomedical areas to discover more information hidden in the microscopic medical images. The segmentation technique is divided into three categories thresholding, boundary_based and region_based segmentation [13]. The threshold is a predefined or computed value selected for dividing the image into collections of pixels with their gray-level values are higher than threshold and collections of pixels and their pixel values are smaller than the threshold. The boundary-based segmentation is based on edges between regions. Most of the edge detection algorithms are based on the changes of the gradient values, for example, the Sobel method [14]. The region-based segmentation method is based on similarities between regions. The region growing algorithm partition an image by joining the neighbor pixels based on similarity criteria [15]. In this paper, we have implemented threshold-based image-segmentation, boundary-based image-segmentation and region-based segmentation techniques and concluded the accuracy of segmentation using segmentation evaluation metrics.

II. SEGMENTATION METHODS

Image-segmentation plays a key function in extracting meaningful information from an image for all kind of microscopic medical image applications.

Manuscript published on 30 September 2019.
***Correspondence Author(s)**
L. Prabaharan*, School of Computing, SASTRA UNIVERSITY, Thanjavur, India. Email: prabaharanl@yahoo.com
A. Sivapathi, School of Computing, SASTRA UNIVERSITY, Thanjavur, India. Email: sivapathi@gmail.com
Dr. A. Raghunathan, AGM (Retd.), Bharath Heavy Electricals Ltd., Trichy, India. Email: arnathan59@gmail.com

Retrieval Number: K22410981119/19©BEIESP
DOI: 10.35940/ijitee.K2241.0981119
Journal Website: www.ijitee.org

Published By:
Blue Eyes Intelligence Engineering and Sciences Publication (BEIESP)

This is one among the most vital steps to get into Image-Understanding, Image-Analysis and Image-Interpretation. We have used Visual Studio 2008 VB.Net for formulating the code for various global thresholding techniques such as Mean threshold, Kapur Entropy threshold, Moments threshold and Otsu's threshold. We also used ImageJ tool for getting optimum threshold value based on Renyi threshold, Minimum threshold, Triangle threshold and Yen threshold. Based on these implementations, we have got a better result for

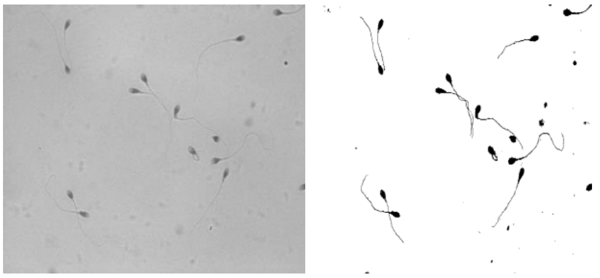

(a) Original image (b) Ground Truth image with threshold value is 167

Fig.:2 Human spermatozoa cell

finding the optimum threshold value for the better segmentation process.

A. Thresholding

One of the important and simple segmentation methods is thresholding. Only single thresholding value is selected for the entire image. Let f(x,y) be an image with the highest pixel value I_{high} and T represents the percent threshold of highest pixel-value above which the pixels can be selected, pixels with value p given by

$$\frac{T}{100} I_{high} \leq p \leq I_{high} \quad (1)$$

A black and white (binary) image g(x,y) can be formulated as

$$g(x,y) = \begin{cases} 1 & \text{if } f(x,y) \geq p \\ 0 & otherwise \end{cases} \quad (2)$$

In which pixels with value 1 belong to the foreground that is Region of Interest, pixels with gray level value 0 related to the background. Global thresholding performs well for the images having a more significant difference between foreground and background. But it is not applicable for images with more than one object having overlapping intensity levels. Normally the threshold selection is difficult due to the images with low contrast or over group of regions in an image.

Selection of threshold value for an image-segmentation is also based on the statistical analysis of the pixel distribution in the image. The authors of [16] have categorized the thresholding methods into six groups such as histogram shape-based, clustering, entropy, object attribute, spatial methods and hybrid methods. We have tried the various global thresholding methods such as Mean, Entropy (Kapur), Otsu, Triangle, Minimum, moments, Renyi and Yen Thresholding (depicted in Fig.:3) on microscopic sperm cell images and compared their pixel distributions with pixel distributions of resultant images shown in Table 1.

The pixel distribution analysis can give an accurate report about the segmentation process. The authors of various research works have introduced different techniques based on pixel distribution for selecting threshold value for the image segmentation. According to our naked eye analysis about the mean thresholding for the input image is not segmented well, and unwanted information was also extracted. The Fig.: 3 show the resultant images of global thresholding. The original image of human spermatozoa is given in the Fig.: 2(a) and ground truth image is depicted in Fig.: 2(b). The ground truth image has been given here for the comparison of better segmentation. The actually expected segmentation can be seen through ground truth images for the purpose of manual naked eye verification.

We have used the sample microscopic medical images of human spermatozoa taken from the gold standard database available as an online source [18]. All sample images have been converted into 8-bit tiff formatted images for all segmentation methods.

B. Mean Thresholding

The threshold value can be computed based on the mean of image pixels. From the image histogram, we have calculated the mean as a threshold value for dividing the image into two clusters of pixels as background and foreground. This thresholding method is normally applied to all type of images for segmentation. The mean value for the input image was 185. This value is not satisfying our expectation for the image segmentation, shown in Fig.:3.

$$\mu = \frac{1}{n} \sum_{i=0}^{n-1} \mathrm{p(i)} \quad (3)$$

C. Otsu's Thresholding

One of the most referenced clustering thresholding is Otsu's thresholding, which divides the image into two sections (classes) so that the variance within each division is minimized. The selection of the threshold value modifies the width of the distribution of two classes. The intention is to select the threshold value that minimizes the combined width of two distributions. The intra_class and inter_class variance are to be computed in order to find the optimum thresholding for the segmentation process. The inter_class variance is computed by subtracting the intra_class variance from the total variance.

$$\sigma^2{}_{\mathrm{intra}}(\mathrm{T}) = \mathrm{n_{BG}(T)}\sigma^2{}_{\mathrm{BG}}(\mathrm{T}) + \mathrm{n_{FG}(T)}\sigma^2{}_{\mathrm{FG}}(\mathrm{T}) \quad (4)$$

Where

$$n_{BG}(T) = \sum_{i=0}^{\mathrm{T}-1} \mathrm{p(i)} \quad (5)$$

$$n_{FG}(T) = \sum_{i=T}^{\mathrm{N}-1} \mathrm{p(i)} \quad (6)$$

$$\sigma^2{}_{\mathrm{BG}}(\mathrm{T}) = \text{The variance of background pixels.} \quad (7)$$

$$\sigma^2{}_{\mathrm{FG}}(\mathrm{T}) = \text{The variance of foreground pixels.} \quad (8)$$

$$\sigma^2{}_{\mathrm{inter}}(\mathrm{T}) = \sigma^2 - \sigma^2{}_{\mathrm{intra}}(\mathrm{T}) \quad (9)$$

We have implemented Otsu's thresholding on the image data set and retrieved the resultant image, which is given in Fig.:3. Otsu's technique acquires a threshold value based on the minimized variance of the image histogram, which was not suitable for this kind of images. The pixels of the region of interest were not extracted well according to our expectation.

D. Entropy-based Thresholding

Entropy was introduced by Shannon to measure the data transmission over a noisy channel.

Retrieval Number: K22410981119/19©BEIESP
DOI: 10.35940/ijitee.K2241.0981119
Journal Website: www.ijitee.org

Published By:
Blue Eyes Intelligence Engineering
and Sciences Publication (BEIESP)

High entropy means great data transmission. Kapur et al. applied Shannon's entropy on an image to calculate and sum the entropy for foreground and background classes. If the sum is maximum, then the threshold is optimum.

Table: 1 Statistical information of various global thresholding				
Type of Segmentation	**Mean Threshold**	**Entropy (Kapur) Threshold**	**Moments Threshold**	**Otsu Threshold**
Threshold value:	185	160	177	184
Foreground pixels: (object)	196283	3832	27845	196223
Background pixels:	256117	448568	424555	256177
Minimum intensity	50	50	50	50
Maximum intensity	218	218	218	218

The probability distribution of a gray level of an image is calculated. The probability distribution for the Foreground pixels can be

$$p_0/P_{BG}, p_1/P_{BG}, \ldots p_t/P_{BG}, \quad (10)$$

for Background pixels

$$(p_{t+1})/1-P_{BG}, (p_{t+2})/1-P_{BG}, \ldots (p_{n-1})/1-P_{BG}, \quad (11)$$

Where 't' is the thresholding value, 'pi' is the probability value of pixels at gray level i, and P_{BG} is the probability of gray level less than or equal to the threshold.

$$P_{BG} = \sum_{i=0}^{t} p_i \quad (12)$$

The entropy of the pixels belong to an object (foreground) of image is

$$P_{FG} = -\sum_{i=0}^{t} p_i/P_{BG} \log (p_i/P_{BG}) \quad (13)$$

The entropy of the background is

$$P_{BG} = -\sum_{i=t+1}^{n-1} p_i/(1-P_{BG}) \log\left(\frac{p_i}{-P_{BG}}\right) \quad (14)$$

The threshold 't' is selected such that the total entropy $P_{BG} + P_{FG}$ is maximized. This method has given optimum thresholding value for the segmentation of human spermatozoa image. Comparing to other methods, this method of thresholding is suitable for microscopic medical images. The resultant segmented images are given in the Fig.:3 and Fig.:4.

E. Moments Thresholding

The next method of global thresholding is Moments thresholding. Moment preserving is the process of preserving gray moments of the original image. To transform the pixels of the original image into some other form without losing the generality. This moment can be either a weighted average of pixels or the mass of the intensities. The intention is to cluster the pixels and represent gray level pixel values by a representative for each cluster. This method is based on the attribute similarity. The thresholding method establishes the value by matching the first three gray-level moments with the first three moments of a binary image. The output for this thresholding technique has given a value which is greater than other global thresholding methods. Hence, this method is not suited for this kind of microscopic medical images. The segmented images are shown in the Fig.:3.

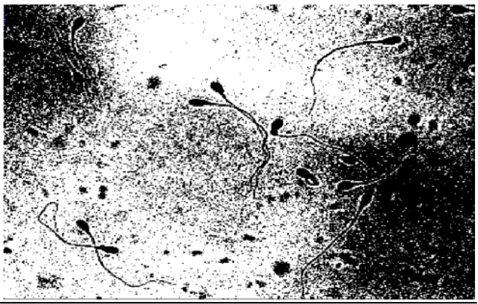

(a) Mean Thresholding-Threshold value is 185

(b) Entropy (Kapur) Thresholding - Threshold value is 160

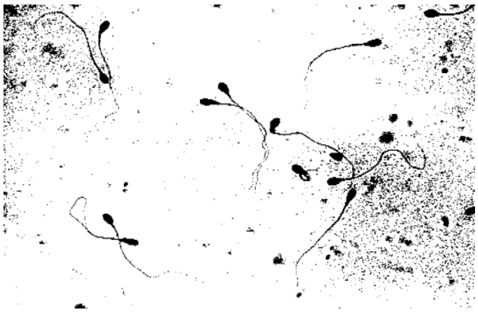

(c) Moments Thresholding - Threshold value is 177

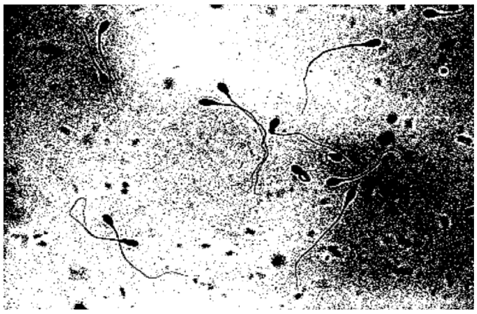

(d) Otsu Thresholding - Threshold value is 184

Fig.:3 Results of various global thresholding

III. METHOD OF ANALYSIS ON SEGMENTATION

As per the manual evaluation, the resultant images given in the Fig.:3 (a-d) and Fig.:4 (a-d) are somewhat matched with the ground truth image (given in the Fig.:2(b)).

Retrieval Number: K22410981119/19©BEIESP
DOI: 10.35940/ijitee.K2241.0981119
Journal Website: www.ijitee.org

Published By:
Blue Eyes Intelligence Engineering and Sciences Publication (BEIESP)

Table: 2 Statistical information of various global thresholding

Type of Segmentation	Minimum Threshold	Renyi Threshold	Triangle Threshold	Yen Threshold
Threshold value:	126	186	171	184
Foreground pixels: (object)	1580	228395	7665	196223
Background pixels:	450820	224005	444735	256177
Minimum intensity	50	50	50	50
Maximum intensity	218	218	218	218

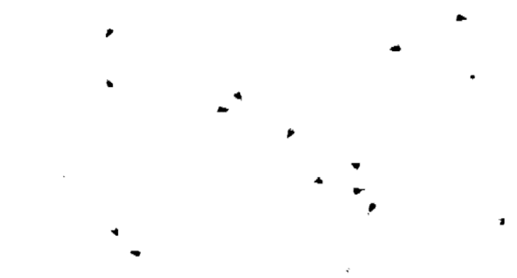

(a) Minimum Thresholding - Threshold value is 126

(b) Renyi Entropy Thresholding - Threshold value is 159

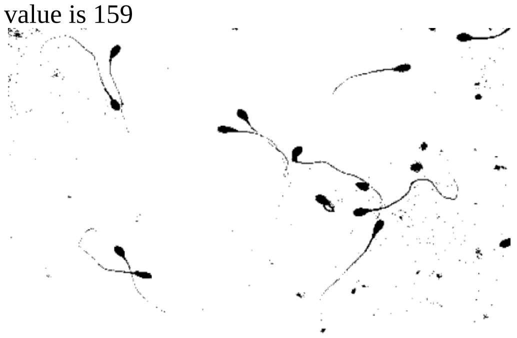

(c) Triangle Thresholding - Threshold value is 184

(d) Yen Thresholding - Threshold value is 171

Fig.:4 Results of various global thresholding

Out of eight segmentation methods under global thresholding, the entropic thresholding is closer to the desired thresholding.

The objects have been extracted nearly and the unwanted background pixels were excluded almost. The entropy-based segmentation works on the basis of the probability density of the region of interest. There are many researchers have considered the probability density of foreground and background pixels and made a lot of updates in entropic thresholding.

We have analyzed the frequency of each pixel through histograms of the input image (Fig.5) shown in the Table:3. The histogram was divided into four quadrants based their minimum gray level and maximum gray level. The minimum gray level was 50 and the maximum gray level was 218. The frequency percentage of Gray level between 0 and 55 was zero percent. There was 0.196 percentage of pixels fall on gray level 56 to 111. The frequency percentage of gray level between 112 and 157 was 0.7488 % and remaining 99.054 % of pixels fall on a gray level from 158 to 223. The analysis result showed that the desired threshold value would be between 163 and 169. The Fig.: 6 show the thresholding values retrieved by using various global thresholding methods and given along with the desired thresholding value. We have already retrieved the expected thresholding value by manual selection and showed its extraction result in Fig.2(b).

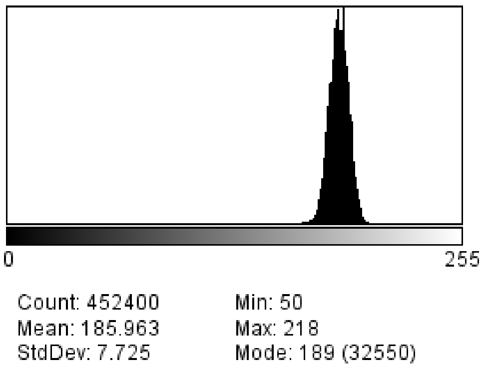

Fig.:5 Histogram of Fig.:1

Table:3 Histogram analysis of Fig.:1

Percentage of pixel distribution	
Gray Level	Frequency Percentage
0- 55	0
56-111	0.19672856
112-157	0.74889478
158-223	99.0543767

Retrieval Number: K22410981119/19©BEIESP
DOI: 10.35940/ijitee.K2241.0981119
Journal Website: www.ijitee.org

Published By:
Blue Eyes Intelligence Engineering
and Sciences Publication (BEIESP)

OPEN ACCESS
International Journal of Innovative Technology and Exploring Engineering (IJITEE)
ISSN: 2278-3075 (Online), Volume-8 Issue-11, September 2019

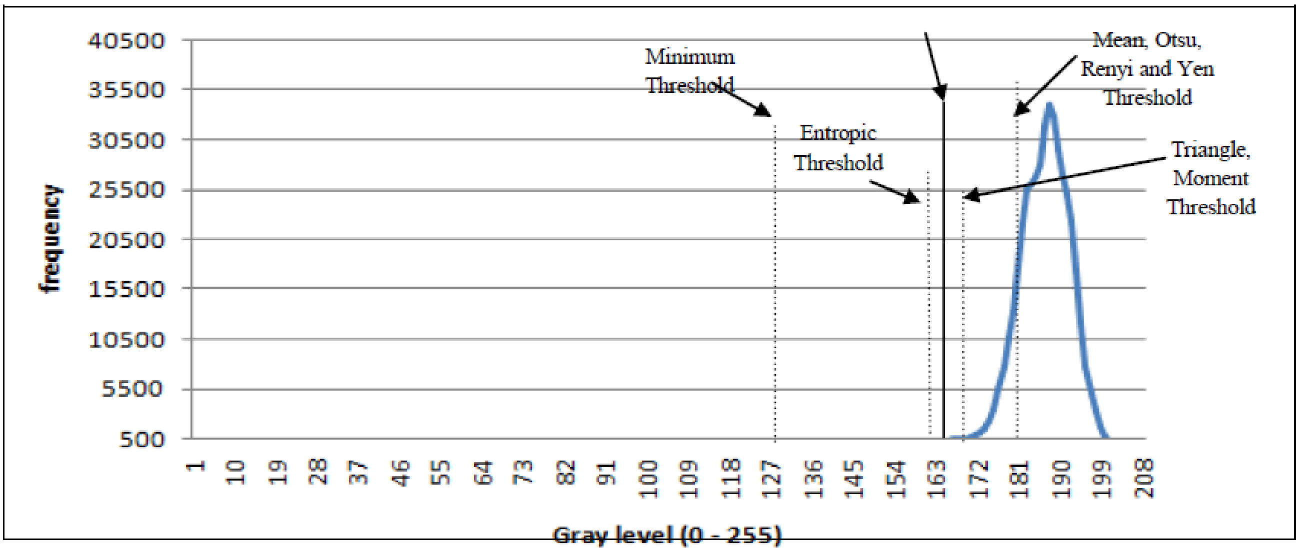

Fig.:6 Thresholding values of Various global thresholding and the desired threshold value.

IV. PERFORMANCE ANALYSIS

The performance of various global thresholding techniques can be measured with the help of segmentation metrics such as specificity, precision, kappa, accuracy, recall, true positive rate, Dice, supervised metrics (misclassification error and Relative foreground area error) and un-supervised metrics (Dwr-minimum value and non- uniformity). We have used D_{WR} and Non-Uniformity metrics to measure the quality of threshold-based segmentation. The D_{WR} metric is measuring the differences between the pixels of the original image and resultant image. The D_{WR} is analyzing the gray level error as follows

$$Discrepancy = \sum_{i}^{h}\sum_{j}^{w}(O(i,j) - S(i,j)) \qquad (15)$$

Where O(i,j) is the gray-level value of picture element p(i,j) on original image and S(i,j) is the gray level value of Segmented image. The discrepancy report is given for all segmentation method. According to this report, the entropic threshold (Kapur) based segmentation is worked well on microscopic sperm cell images is given in the Table:4.

Table:4 Accuracy measuring of various segmentation methods using D_{WR} metric.

Segmentation method	Metric Result
Entropy (Kapur)	-30622784
Yen Threshold	-30325745
Renyi Threshold	-30059744
Triangle Threshold	-29082329
Moments Threshold	-23936429
Minimum Threshold	-19795819
Mean Threshold	947914
Otsu Threshold	10687981

To ensure the previous performance analysis, we have taken the Non-Uniformity metric to measure the quality of segmentation performances of various global thresholding methods. The Non-Uniformity (NU) is given in equation (16), where σ_f^2 represents the foreground variance of the segmented image. σ^2 represents the whole variance of the segmented image. FG and BG are the pixels of the foreground and background area of the segmented image. This metric evaluates the segmented image based on their foreground and background variances. The Non-Uniformity value is close to zero means the particular image is segmented well. The report is given in the Table:5, which shows that the Entropic thresholding (Kapur) is better than all other thresholding methods. The Minimum thresholding method has lost some of the ROI in the segmented image and has yielded threshold value as 126, which is very far from the desired thresholding (given in Fig:5).

$$NU = \frac{|FG|\sigma_f^2}{|FG+BT|\ \sigma^2} \qquad (16)$$

Table:5 Accuracy measuring of various segmentation methods using Non-Uniformity metric

Segmentation method	Metric Result
Minimum Threshold	0.0021
Entropy (Kapur)	0.0204
Renyi Threshold	0.0271
Triangle Threshold	0.1151
Mean Threshold	0.6265
Moments Threshold	0.7430
Otsu Threshold	4.2808
Yen Threshold	28.2280

V. CONCLUSION

We have tried and achieved significant remarks on segmenting medical microscopic sperm cell images using various global thresholding methods. We have identified that the entropic thresholding method has extracted the ROI as expected from the ground truth. It is proved that the entropic thresholding has given the threshold value, which is close to the desired thresholding. We would like to widen our study on the entropic thresholding to get the desired threshold value for the proper segmentation and further feature extraction.

REFERENCES

1. Rintu Maria Thomas, Jisha John, "A review on cell detection and segmentation in microscopic images", International Conference on Circuits, Power and Computing Technologies [ICCPCT] – 2017.
2. Srinivasan Sankaran, Muthukumaran Malarvel, Gopalakrishnan Sethumadhavan, Dinkar Sahal, "Quantitation of Malarial parasitemia in Giemsa stained thin blood smears using Six Sigma threshold as preprocessor" - Optik 145 (2017) 225–239

3. K.Stouffs, H. Tournaye, J. Van der Elst, I.Liebaers, W.Lissens, “Is there a role for the nuclear export factor2 gene in male infertility? Fertile. Sterile”. 90 (2008) 1787- 1791.
4. L.Prabaharan, A.Raghunathan, “De-noising filters for microscopic medical images of human spermatozoa” –Journal of Theoretical and Applied Information Technology- 15th January 2018. Vol.96. No 1.
5. Bhupendra S. Deshmukh, Vijay H. Mankar, “Segmentation of Microscopic Images: A Survey” International Conference on Electronic Systems, Signal Processing and Computing Technologies, 2014- 978-1-4799-2102-7/14.
6. X. Chen, X. Zhou, and S.Wong, "Automated segmentation, classification, and tracking of cancer cell nuclei in time-lapse microscopy," *IEEE Transactions on Biomedical Engineering*, vol. 53, no. 4, pp. 762–766, 2006
7. F. Yang, M. A. Mackey, and F. Lanzini, “Cell segmentation, tracking, and mitosis detection using temporal context,” in *Medical Image Computing and Computer-Assisted Intervention*, 2005, pp. 302–309.
8. K. Jiang, Q. Liao, and S. Dai, “A novel white blood cell segmentation scheme using scale-space filtering and watershed clustering,” in *International Conference on Machine Learning and Cybernetics*, 2003, pp. 2820–2825.
9. S. Farnoosh and S. Zainina, “A framework for white blood cell segmentation in microscopic blood images using digital image processing,” *Biological Procedures Online*, vol. 11, no. 1, pp. 196–206, 2009.
10. A. K. Jain, S. P. Smith, and E. Backer, “Segmentation of muscle cell pictures: a preliminary study,” *IEEE Transactions on Pattern Analysis and Machine Intelligence*, vol. 12, no. 3, pp. 232–242, 1980.
11. G. Lin, U. Adiga, and K. Olson, “A hybrid 3D watershed algorithm incorporating gradient cues and object models for automatic segmentation of nuclei in confocal image stacks,” *Cytometry Part A*, vol. 56, no. 1, pp. 23–36, 2003.
12. Neerad Phansalkart, Sumit More, Ashish Sabale Madhuri Joshi “Adaptive Local Thresholding for Detection of Nuclei in Diversity Stained Cytology Images” *978-1-4244-9799-7/11, IEEE* 2011.
13. K. Fu and JK. Mui, “A survey on image segmentation,” *Pattern Recognition*, vol. 13, no. 1, pp. 3 16, 1981
14. I. Sobel, “History and definition of the Sobel operator,” 2014
15. J. Fan, D. K. Y. Yau, A. K. Elmagarmid, and W. G. Aref, “Automatic image segmentation by integrating color edge extraction and seeded region growing,” *IEEETransactions On Image Processing*, vol. 10, pp. 1454–1466, 2001.
16. Mehmet Sezgin and Bulent Sankur, “Survey over image thresholding techniques and quantitative performance evaluation”, Journal of Electronic Imaging 13(1), 146–165 (January 2004).
17. DM Carabias, “Analysis of image thresholding methods for their application to augmented reality environments”, https://eprints.ucm.es/16932/1/Tesis_Master_Daniel_Martin_Carabias.pdf, 2012.
18. http://morfologia.cedai.cl/public